



Verification of Numerical Models for Pressure Hull Collapse Predictions

John R. MacKay

Defence R&D Canada – Atlantic

Technical Memorandum
DRDC Atlantic TM 2011-281
November 2011

This page intentionally left blank.

Verification of Numerical Models for Pressure Hull Collapse Predictions

John R. MacKay

Defence R&D Canada – Atlantic

Technical Memorandum

DRDC Atlantic TM 2011-281

November 2011

Principal Author

Original signed by John R. MacKay

John R. MacKay

Defence Scientist, Warship Performance

Approved by

Original signed by Neil G. Pegg

Neil G. Pegg

Head, Warship Performance

Approved for release by

Original signed by Calvin V. Hyatt

Calvin V. Hyatt

Chair, Document Review Panel

© Her Majesty the Queen in Right of Canada, as represented by the Minister of National Defence, 2011

© Sa Majesté la Reine (en droit du Canada), telle que représentée par le ministre de la Défense nationale, 2011

Abstract

The verification aspects of a verification and validation (V&V) study for the numerical modeling of the collapse of pressure hulls are described. A series of finite element (FE) analyses were performed using ANSYS in order to verify that the numerical methodology was correctly implemented in the software (code verification) and that spatial and temporal refinement of validation FE models of test specimens were adequate (calculation verification). FE predictions of elastic and inelastic buckling pressures for 140 cylinders and ring-frames under external pressure were found to be within 8%, on average, of the benchmark analytical or numerical solutions. The FE error was attributed to unavoidable differences between the numerical and benchmark models, rather than problems with the FE software, so that code verification was considered to have been achieved. With calculation verification, the nonlinear FE solution was found to be most sensitive to the spatial refinement associated with the mesh density. Load increment size was found to affect the collapse prediction to a lesser extent, and the tolerance used to define convergence of the incremental solution did not affect the collapse prediction at all when a refined mesh and load increment were used. The outcomes of the calculation verification study were a standard mesh density, load increment size and convergence tolerance that can be used for further validation analyses of test specimens, and for future FE analyses of pressure hulls.

Résumé

Les aspects de vérification d'une étude de vérification et de validation (V et V) pour la modélisation numérique de l'écrasement de coques épaisses sont décrits. Une série d'analyses par éléments finis ont été effectuées à l'aide du logiciel ANSYS dans le but de vérifier si la méthodologie numérique a bien été implantée dans le logiciel (vérification des codes) et si le raffinement spatial et le raffinement temporel des modèles de validation par éléments finis des spécimens d'essais étaient adéquats (vérification des calculs). Les prédictions par éléments finis des pressions de flambage élastique et inélastique pour 140 cylindres et cadres de fuselage sous pression externe sont d'environ 8 %, en moyenne, des solutions analytiques ou numériques de référence. L'erreur par éléments finis a été attribuée à des différences inévitables entre les modèles numériques et les modèles de référence, plutôt qu'à des problèmes avec le logiciel d'analyse par éléments finis, ce qui fait en sorte que la vérification des codes a été considérée comme effectuée. Avec la vérification des calculs, la solution d'éléments finis non linéaire a été jugée la plus sensible pour le raffinement spatial associé à la densité de mailles. Il a été déterminé que la variation de charge a une faible incidence sur la prédiction d'écrasement et que la tolérance utilisée pour définir la convergence de la solution de variation n'a aucune incidence sur la prédiction d'écrasement lorsqu'un maillage raffiné et une variation de charge sont utilisés. Les résultats de l'étude de vérification des calculs étaient une densité des mailles standard, une variation de la charge standard et une tolérance de convergence standard, qui peuvent être utilisées pour de futures analyses de validation des spécimens d'essais et pour de futures analyses par éléments finis de coques épaisses.

This page intentionally left blank.

Executive summary

Verification of Numerical Models for Pressure Hull Collapse Predictions

John R. MacKay; DRDC Atlantic TM 2011-281; Defence R&D Canada – Atlantic; November 2011.

Introduction: DRDC Atlantic is developing a partial safety factor (PSF) and accompanying numerical modeling rules for finite element (FE) predictions of the collapse of pressure hulls. DRDC has adopted a verification and validation (V&V) methodology in order to establish credibility and confidence in the numerical modeling through comparisons of numerical and experimental results. The current technical memorandum describes verification aspects of the V&V study. A series of FE analyses were performed using ANSYS in order to verify that the numerical methodology is correctly implemented in the software (code verification) and that spatial and temporal refinement of validation FE models of test specimens are adequate (calculation verification).

Results: FE predictions of elastic and inelastic buckling pressures for 140 cylinders and ring-frames under external pressure were found to be within 8%, on average, of the benchmark analytical or numerical solutions. The FE error was attributed to unavoidable differences between the numerical and benchmark models, rather than problems with the FE software, so that code verification was considered to have been achieved. With calculation verification, the nonlinear FE solution was found to be most sensitive to the spatial refinement associated with the mesh density. Load increment size was found to affect the collapse prediction to a lesser extent, and the tolerance used to define convergence of the incremental FE solution did not affect the collapse prediction at all when a refined mesh and load increment were used.

Significance: The verification studies described herein provide assurance that the ANSYS software, which is frequently used by DRDC to assess pressure hulls, has correctly implemented the underlying mathematical and physical models required to predict hull collapse. A standard mesh density, load increment size and convergence tolerance were established for the validation FE analyses that will be used to develop a PSF. Those standard parameters may also be used in future analyses of pressure hulls. Furthermore, the verification framework established herein could be used to verify other software codes, such as DRDC's SubSAS structural modeling and analysis tool.

Future plans: DRDC Atlantic has completed 47 validation FE analyses of pressure hull test specimens using ANSYS. The results of those simulations, as well as ongoing analyses for more recent tests, will be used to quantify the accuracy of the FE methodology and develop a PSF that can be used with numerical collapse predictions.

Sommaire

Verification of Numerical Models for Pressure Hull Collapse Predictions

John R. MacKay; DRDC Atlantic TM 2011-281; R & D pour la défense Canada – Atlantique; Novembre 2011.

Introduction : RDDC Atlantique élabore un facteur de sécurité partiel et des règles de modélisation numérique connexes pour des prédictions par éléments finis de l'écrasement de coques épaisses. RDDC a adopté une méthodologie de vérification et de validation (V et V) dans le but d'établir la crédibilité de la modélisation numérique au moyen de comparaisons des résultats numériques et expérimentaux. Le présent document technique décrit les aspects de vérification de l'étude de V et V. Une série d'analyses par éléments finis ont été effectuées à l'aide du logiciel ANSYS afin de vérifier si la méthodologie numérique a bien été implantée dans le logiciel (vérification des codes) et si le raffinement spatial et le raffinement temporel des modèles de validation par éléments finis des spécimens d'essais étaient adéquats (vérifications des calculs).

Résultats : Les prédictions par éléments finis des pressions de flambage élastique et inélastique pour 140 cylindres et cadres de fuselage sous pression externe sont d'environ 8 %, en moyenne, des solutions analytiques ou numériques de référence. L'erreur par éléments finis a été attribuée à des différences inévitables entre les modèles numériques et les modèles de référence, plutôt qu'à des problèmes avec le logiciel d'analyse par éléments finis, ce qui fait en sorte que la vérification des codes a été considérée comme effectuée. Avec la vérification des calculs, la solution d'éléments finis non linéaire a été jugée la plus sensible pour le raffinement spatial associé à la densité de mailles. Il a été déterminé que la variation de charge a une faible incidence sur la prédiction d'écrasement et que la tolérance utilisée pour définir la convergence de la solution de variation n'a aucune incidence sur la prédiction d'écrasement lorsqu'un maillage raffiné et une variation de charge sont utilisés.

Importance : Les études de vérification décrites dans le présent document garantissent que le logiciel ANSYS, qui est souvent utilisé par RDDC pour évaluer les coques épaisses, a bien implanté les modèles mathématiques et physiques sous-jacents nécessaires pour prédire l'écrasement de la coque. Une densité des mailles standard, une variation de la charge standard et une tolérance de convergence standard ont été établies pour les analyses par éléments finis de validation qui seront utilisées pour mettre au point un facteur de sécurité partiel. Ces paramètres standard peuvent également être utilisés lors des futures analyses de les coques épaisses. De plus, le cadre de vérification établi dans le présent document pourrait être utilisé pour vérifier d'autres codes de logiciel, comme l'outil d'analyse et de modélisation de structure SubSAS de RDDC.

Perspectives : RDDC Atlantique a effectué 47 analyses par éléments finis de validation des spécimens d'essais de la coque épaisse à l'aide du logiciel ANSYS. Les résultats de ces simulations, ainsi que des analyses en cours pour des essais plus récents, seront utilisés pour quantifier la justesse de la méthodologie par éléments finis et pour mettre au point un facteur de sécurité partiel qui pourra être utilisé avec les prédictions numériques de l'écrasement de coques épaisses.

Table of contents

Abstract	i
Résumé	i
Executive summary	iii
Sommaire	iv
Table of contents	v
List of figures	vi
List of tables	vii
1 Introduction.....	1
2 Code Verification.....	3
2.1 Elastic Buckling of a Cylindrical Shell	3
2.2 Elastic Buckling of a Ring-Stiffened Cylinder.....	6
2.3 Elasto-Plastic Collapse of a Ring-Frame.....	9
3 Calculation Verification.....	13
3.1 Example Test Specimen	13
3.2 Mesh Density.....	15
3.3 Load Increment Size.....	16
3.4 Solution Convergence Tolerances	18
4 Conclusions.....	20
References	21
Annex A .. Standard Numerical Methodology.....	23
List of symbols/abbreviations/acronyms/initialisms	25
Distribution list.....	27

List of figures

Figure 1: Results of a verification study based on the elastic buckling of a simply-supported cylindrical shell under external pressure. The classical solution is based on Kendrick's iterated solution for the von Mises pressure. Note the logarithmic scale for both axes.	4
Figure 2: FE mesh (a) and predicted buckling mode (b) for a cylinder shell.	5
Figure 3: Results of a mesh convergence study for the elastic buckling of a simply-supported cylindrical shell under external pressure.	5
Figure 4: Results of a verification study based on the elastic buckling of a simply-supported ring-stiffened cylinder under external pressure.	7
Figure 5: FE mesh (a) and predicted buckling mode (b) for a ring-stiffened cylinder with $L_B L_f^{-1}=11$ and $d=f=9$ mm.	8
Figure 6: Results of a mesh convergence study for the elastic buckling of a simply-supported ring-stiffened cylinder under external pressure.	8
Figure 7: Results of a verification study based on the elasto-plastic overall collapse of an infinitely long ring-stiffened cylinder under external pressure.	11
Figure 8: FE mesh (a) and predicted buckling mode (b) for a ring-frame with $\sigma_y=150$ MPa and $\epsilon_{ps} a^{-1}=0.1\%$	11
Figure 9: Nominal axisymmetric geometry of specimen L510-No18 [17]. All dimensions are in millimetres.	13
Figure 10: Graphical representation of out-of-circularity of specimen L510-No18. The colour contour maps describe the radial eccentricity (mm) based on a double Fourier analysis of the measurements of the outer shell taken by the CMM. The out-of-circularity is also indicated by the deformed shape of the model, whereby the imperfections are magnified by a factor of 50.	14
Figure 11: A photograph of specimen L510-No18 after collapse testing (left), and the collapse shape predicted using the standard FE methodology in Annex A.	14
Figure 12: Results of a mesh convergence study for L510-No18, showing the predicted collapse pressure versus the total number of elements in the FE model.	15
Figure 13: Pressure-displacement curve predicted by nonlinear FE analysis for L510-No18. The FE model is based on Mesh H, with an initial load increment of 1.0 MPa. The plotted displacement corresponds with the maximum deformation for the predicted collapse shape.	17
Figure 14: Results of a load increment size study for L510-No18, showing the predicted FE collapse pressure versus the total number of load increments up to the collapse pressure. The initial load increment size corresponding with each analysis is shown on the secondary axis.	18

List of tables

Table 1: Summary of a load increment study for L510-No18.....	16
---	----

This page intentionally left blank.

1 Introduction

Numerical modeling, especially nonlinear finite element (FE) analysis, is an essential element of DRDC Atlantic's toolkit for conducting structural assessments of pressure hulls. Unfortunately, because FE methods have not been properly validated in this context, they can only be used to make qualitative recommendations (e.g. that a load or defect does or does not affect the hull's structural capacity). In some cases, FE results are indirectly used to make quantitative recommendations by comparing FE collapse predictions with and without hull defects and applying the percent difference to the design collapse strength, which is based on the analytical-empirical methods in [1].

What is needed is a partial safety factor (PSF) that can be applied to FE collapse predictions. In that way, the design collapse strength of a pressure hull could be calculated directly from the numerical results. That approach would facilitate the assessment of a variety of hull maintenance and damage issues that affect the hull collapse strength.

DRDC Atlantic is pursuing the development of a partial safety factor and accompanying numerical modeling rules for FE pressure hull collapse predictions. DRDC's approach, which is presented in [2], adopts the verification and validation (V&V) philosophy endorsed by ASME [3]. The goal of V&V is to establish credibility and confidence in a given numerical model for predicting a specific response. That is accomplished by comparing numerical predictions to experimental results, and using those data to estimate the accuracy of the numerical model. The two components of V&V are verification, which involves ensuring a correct numerical implementation of the underlying mathematical model, and validation, which leads to the quantitative accuracy assessment. DRDC aims to take the standard V&V process a step further, by transforming the accuracy assessment into a PSF for design and analysis of pressure hulls.

DRDC's software toolkit for FE modeling of pressure hulls includes the commercial FE code ANSYS [4], an in-house C++ code called CylMesh, which is used to produce pressure hull FE models for analysis by ANSYS, as well as SubSAS [5]. SubSAS is a pressure hull structural modeling tool that was developed specifically for DRDC and the UK MoD by Martec Limited. With SubSAS, the user can generate detailed FE models of pressure hulls, which are then analyzed using the DRDC/Martec FE solver VAST [10]. DRDC aims to validate their full suite of numerical tools, including SubSAS, VAST, CylMesh and ANSYS. The current work is focussed on CylMesh/ANSYS collapse predictions.

The first steps in the V&V process for both CylMesh/ANSYS and SubSAS/VAST are presented in [11], where those programs were used to simulate the collapse of 22 tests specimens from a Canada-Netherlands experimental program for pressure hulls with corrosion damage [12]-[14]. The outcomes of the simulations in [11] were a set of modeling rules for FE collapse predictions, as well as an initial estimate of the numerical accuracy. Both programs were found to predict the experimental collapse pressures with approximately 11% accuracy, with 95% confidence. The remaining 26 test results from the Canada-Netherlands program, which are reported in [15]-[17], will be used in the final V&V accuracy assessment of CylMesh/ANSYS and SubSAS/VAST.

The current technical memorandum presents verification aspects of the CylMesh/ANSYS V&V study. Verification is divided into two streams. Code verification is concerned with checking for

errors in the implementation of the mathematical model in the source code of the numerical software. That is primarily a software development task, since the source code of commercial numerical software, e.g. ANSYS, is not available to the analyst. Nonetheless, the numerical implementation can be indirectly verified by comparing numerical results with analytical solutions or benchmark numerical solutions. Those types of comparisons usually involve simplified, but related idealizations of the actual system being studied. The second part of verification is calculation verification. That involves performing convergence studies on the spatial and temporal discretization of the model in order to ensure that the exact numerical solution, which is not necessarily the correct solution to the problem, is being approached.

This document summarizes the verification studies that were performed with CylMesh/ANSYS as an initial step in formally validating that software for collapse predictions. Code verification involved comparing numerical results with classical analytical solutions for elastic buckling of cylindrical shells and ring-stiffened cylinders, as well as a well-established finite difference solution for the elasto-plastic collapse of a ring-frame. Those studies are presented in Section 2. It is normally assumed that the numerical methods have been correctly implemented in commercial software codes like ANSYS, and so code verification is often neglected. The current work looks at code verification because, on the one hand, it is necessary for a complete and thorough V&V process, and on other the hand, it shows that the numerical implementation is correct for simple problems, thereby reducing the potential sources of error if the later validation work points to a shortcoming in the simulation of more realistic and complex problems.

Code verification need only be performed once for a specific software product and a given problem. Calculation verification, on the other hand, should be performed each time a new structure is analyzed. That is necessary because the appropriate level of mesh refinement depends on the specific geometry being studied, and furthermore, because the level of load increment refinement is related to the strength of the structure. The calculation verification studies presented herein are specific to the test specimens from [15]-[17], which will be used in the validation stages of the current V&V process. Similar studies should be performed each time a new structure is analyzed. Calculation verification included FE mesh convergence studies, which were performed for each unique test specimen configuration. With the current methodology the numerical solution is performed quasi-statically, negating the need for temporal discretization studies. Instead, it was ensured that the load increment size for nonlinear FE analysis was refined sufficiently. Those calculation verification studies are presented in Section 3, along with an investigation of the effect on the collapse prediction of convergence tolerances for the iterative solution procedure. The overall conclusions of the verification study for CylMesh/ANSYS are presented in Section 4.

2 Code Verification

The challenge with code verification is finding exact analytical solutions that can be used to benchmark FE predictions for the problem at hand. After all, numerical models are often used in the first place because the complexity of the problem rules out an exact analytical solution. The compromise is to use analytical solutions to related, but simplified, problems.

The main structural component of a pressure hull is a ring-stiffened cylinder, and so the current problem is the elasto-plastic collapse of ring-stiffened cylinders under external pressure. There are no exact analytical solutions for that problem, even if important factors like out-of-circularity (OOC) shape imperfections are neglected. Code verification was therefore performed for three related problems, as described below.

The first case looked at the elastic buckling of a simply-supported cylindrical shell under external pressure. That problem allowed the basic linear-elastic shell theory, upon which the nonlinear elasto-plastic methodology is built, to be studied. The geometric complexity of the structure was increased with the second case, which considered the elastic buckling of a simply-supported ring-stiffened cylinder under external pressure. With the third and final case, the structural modeling was extended to include nonlinear material and geometry in order to predict the elasto-plastic collapse of an infinitely long ring-stiffened cylinder under external pressure. The three case studies show increasing complexity, with the final problem closely approaching the target problem. On the other hand, it will be shown that the quality of the best available benchmark solutions to those problems diminishes with the complexity of the problem.

Each benchmark solution is briefly described in the following sections. A series of benchmark analytical or numerical models, and FE verification models, were generated for each case. The case studies were designed to cover a range of geometric and/or material parameters in order to verify the FE models over a greater range of interest. The FE modeling was based on the standard CylMesh/ANSYS methodology developed in [11] and summarized here in Annex A. Since the geometry and failure mode for some of the code verification cases differ from a typical pressure hull analysis, some deviations from the standard methodology were required. Those discrepancies are noted in the text.

2.1 Elastic Buckling of a Cylindrical Shell

The governing equations for the elastic buckling of a simply-supported cylindrical shell under external pressure were solved directly by von Mises [18]. The resulting buckling pressure is known as the von Mises pressure, P_{m1} . The current verification task uses a slightly modified version of von Mises' original solution, which is used in the naval design standard in [1]. The modified solution

$$P_{m1} = \frac{Eh}{a} \left[n^2 - 1 + \frac{1}{2} \left(\frac{\pi a}{L} \right)^2 \right]^{-1} \left\{ \left[n^2 \left(\frac{L}{\pi a} \right)^2 + 1 \right]^{-2} + \frac{h^2}{12a^2(1-\mu^2)} \left[n^2 - 1 + \left(\frac{\pi a}{L} \right)^2 \right]^2 \right\} \quad (1)$$

must be minimized by iteration over the circumferential wave number, n , representing the number of complete buckling waves around the cylinder. The axial buckling mode is fixed at one half-wave over the cylinder length ($m=1$). Eq. (1) is valid for a cylinder with length, L , mid-plane radius, a , thickness, h , Young's modulus, E , and Poisson's ratio, μ .

The verification study considered an aluminium tube with the properties shown in Figure 1. Fifty cases were studied by holding the cylinder radius constant and varying its length and thickness. Symmetry in the geometry, loading and displacements allowed the FE models to be reduced so that only half the length and circumference of each cylinder was modeled. The correct response of the quarter-symmetric model was enforced by using appropriate symmetrical boundary conditions. Reduced FE models, like the one shown in Figure 2, significantly decrease computation times compared to whole-cylinder models. Simply-supported boundary conditions were modeled by preventing the end nodes from translating in the radial and circumferential directions. Elastic buckling pressures were predicted using linearized buckling analyses following linear pre-buckling solutions.

One of the verification cases ($aL^{-1}=2, ah^{-1}=200$) was chosen for an FE mesh convergence study. The final FE mesh and predicted buckling mode are shown in Figure 2, and the convergence study is summarized in Figure 3. Each mesh consisted of a uniform grid of approximately square shell elements. The densest mesh, Mesh G, was found to give a buckling pressure within 0.4% of Mesh F. All subsequent analyses used meshes based on the density of Mesh G.

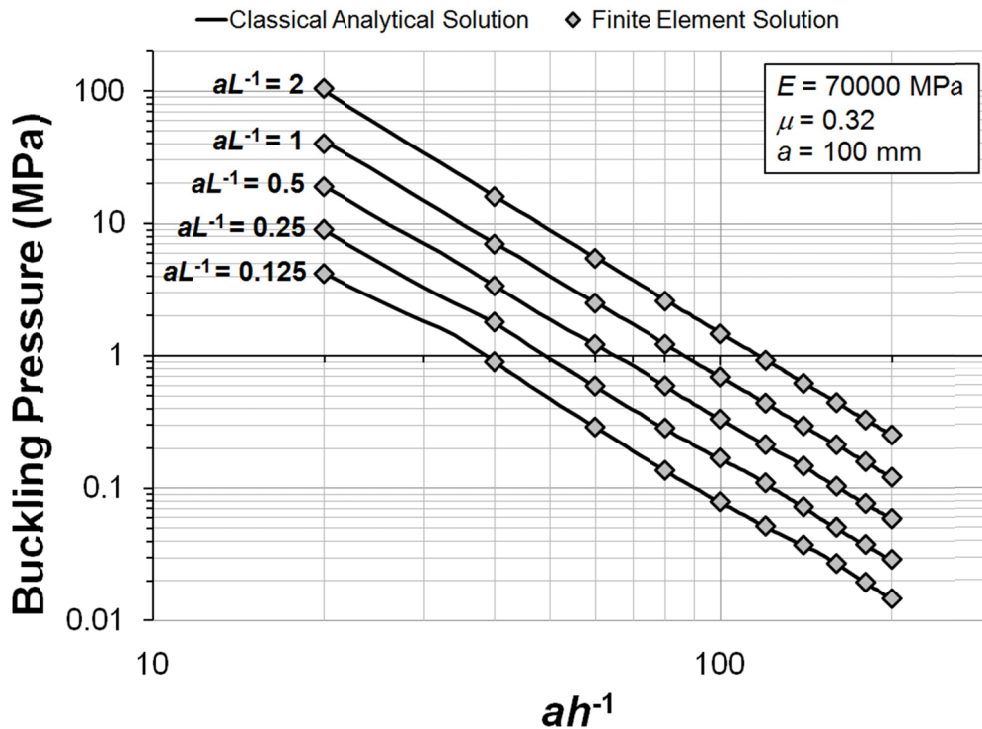


Figure 1: Results of a verification study based on the elastic buckling of a simply-supported cylindrical shell under external pressure. The classical solution is based on Kendrick's iterated solution for the von Mises pressure. Note the logarithmic scale for both axes.

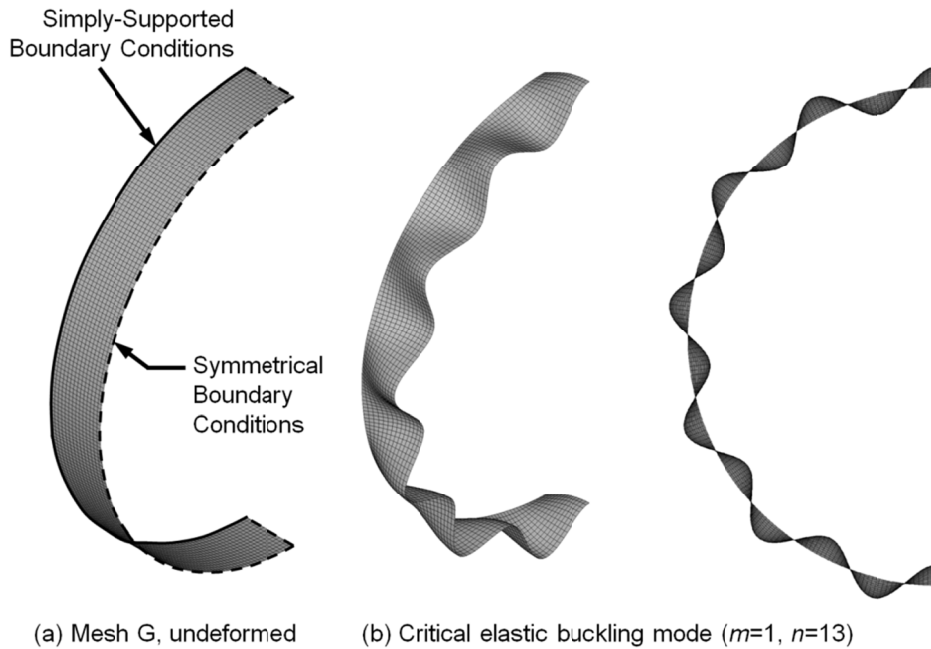


Figure 2: FE mesh (a) and predicted buckling mode (b) for a cylinder shell.

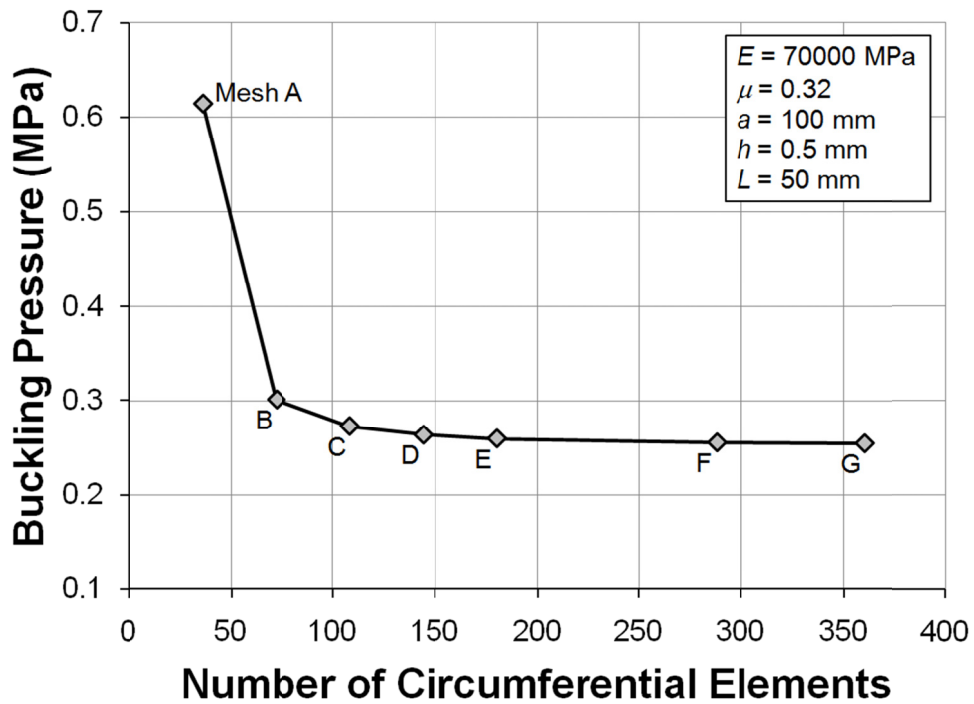


Figure 3: Results of a mesh convergence study for the elastic buckling of a simply-supported cylindrical shell under external pressure.

The results of the verification study are shown in Figure 1, where the predicted buckling pressures are plotted against the ratio of cylinder radius to thickness. Both axes are plotted on logarithmic scales in order to clearly capture the trend over several orders of magnitude in the “slenderness” ratio, ah^{-1} , and buckling pressure. As expected, buckling pressures decrease as the thickness becomes smaller, and as the cylinder length increases.

The FE results in Figure 1 show good qualitative agreement with the analytical results over the entire range of parameters studied. The analytical and FE buckling modes, in terms of the circumferential wave number, n , were in agreement in all cases. The quantitative error can be estimated by taking the root mean square (RMS) of the relative error for each analytical-numerical pair of buckling pressures. The relative error for each case is given by

$$e = \frac{P_{FE} - P_{cl}}{P_{cl}} \quad (2)$$

where P_{FE} and P_{cl} are the numerical and classical analytical buckling pressures, respectively. The RMS error for all cases is taken as

$$\sqrt{\frac{\sum e^2}{N}} \quad (3)$$

for a set of N analytical-numerical comparisons.

The RMS error for the 50 FE results plotted in Figure 1 is 1.5%. The small difference between analytical and numerical results is likely related to the pre-buckling boundary conditions. Von Mises’ solution assumes membrane behaviour, whereby the radial and axial displacements are uniform over the entire cylinder, in the pre-buckling regime; the simply-supported boundary conditions are only applied to the buckling solution. In the FE models, those boundary conditions were applied to both parts of the solution. The FE models were not re-analyzed with membrane assumptions for the pre-buckling solution since the agreement with the classical results was sufficient to verify that the FE models had correctly implemented the linear-elastic shell theory.

2.2 Elastic Buckling of a Ring-Stiffened Cylinder

Kendrick [19] used Ritz’s energy method to find an approximate solution for the elastic buckling pressure of a simply-supported and uniformly ring-stiffened cylinder under external pressure. Kendrick’s derivation involved two important assumptions. First, like von Mises, Kendrick assumed a membrane pre-buckling condition. Second, the ring-stiffeners were assumed to provide only radial support to the shell; the contribution of their torsional stiffness to the bending resistance of the shell was neglected. The buckling mode was defined by trigonometric functions, so that the equations can be solved for an arbitrary combination of m and n . Kendrick’s solution involved finding the determinant of a three-by-three matrix, which resulted from the minimization of the potential energy of the system. The resulting equation for the critical buckling pressure is rather complicated and will not be reproduced here.

FE models were verified against Kendrick's solution in a similar manner as for the von Mises pressure. Sixty aluminium ring-stiffened cylinders were used as the verification case. The geometric and material properties of the cylinders are shown in Figure 4, where L_f is the frame spacing, L_B is the length of the cylinder, h_w is the thickness of the stiffener web, d is the web depth, h_f is the thickness of the stiffener flange, and f is the flange breadth. E , μ , a and h are defined in Section 2.1. The geometries of the cylinders were identical except for the ring-stiffener proportions and the total length of the model. Those parameters were varied in order to examine different failure modes.

The application of simply-supported boundary conditions and the prediction of buckling pressures were carried out in the same way as for the cylindrical shells in Section 2.1. Furthermore, FE models of the ring-stiffened cylinders also used quarter-symmetry model reduction.

The FE models were entirely comprised of shell elements. The ring-stiffeners were modeled with shells, despite the fact that Kendrick treated them as beams with no torsional stiffness in his solution. That discrepancy between the FE and benchmark models is likely to lead to some differences in the buckling predictions, but it was justified because the goal of the verification study is to verify the type of all-shell FE models that will be used in the validation exercise.

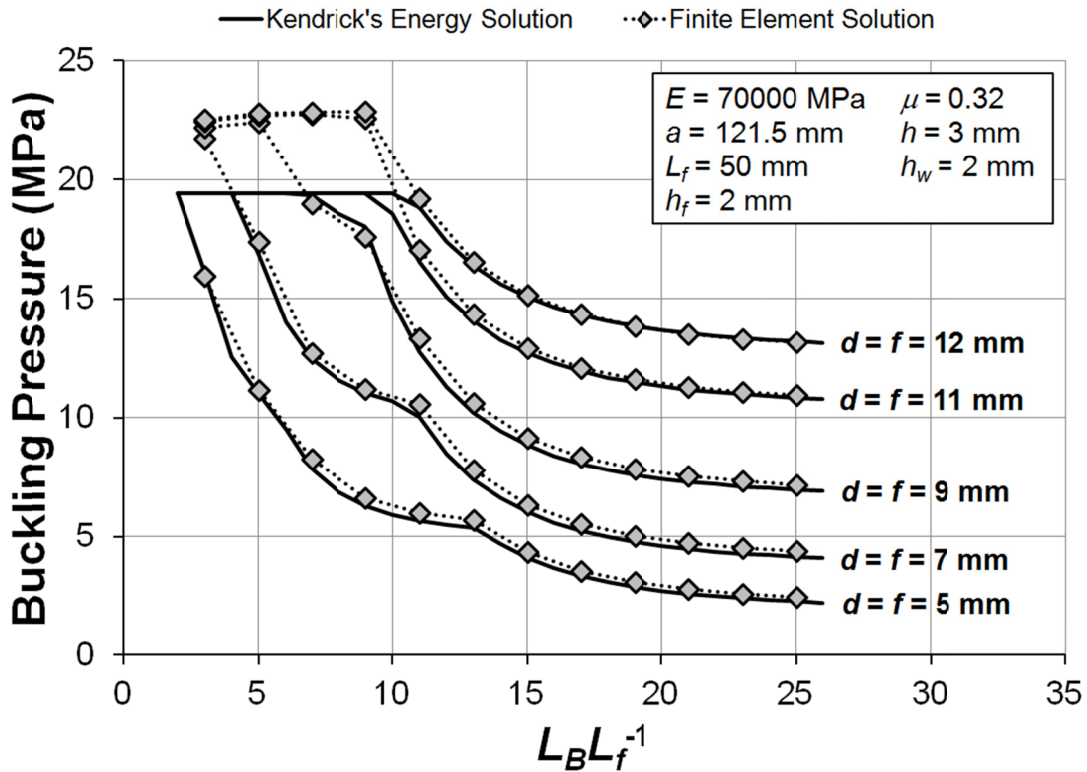


Figure 4: Results of a verification study based on the elastic buckling of a simply-supported ring-stiffened cylinder under external pressure.

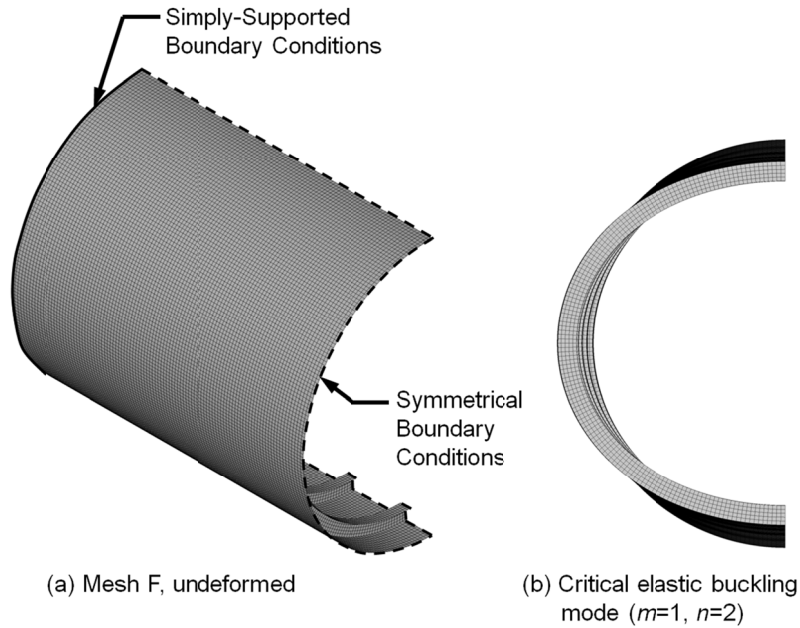


Figure 5: FE mesh (a) and predicted buckling mode (b) for a ring-stiffened cylinder with $L_B L_f^{-1} = 11$ and $d = f = 9$ mm.

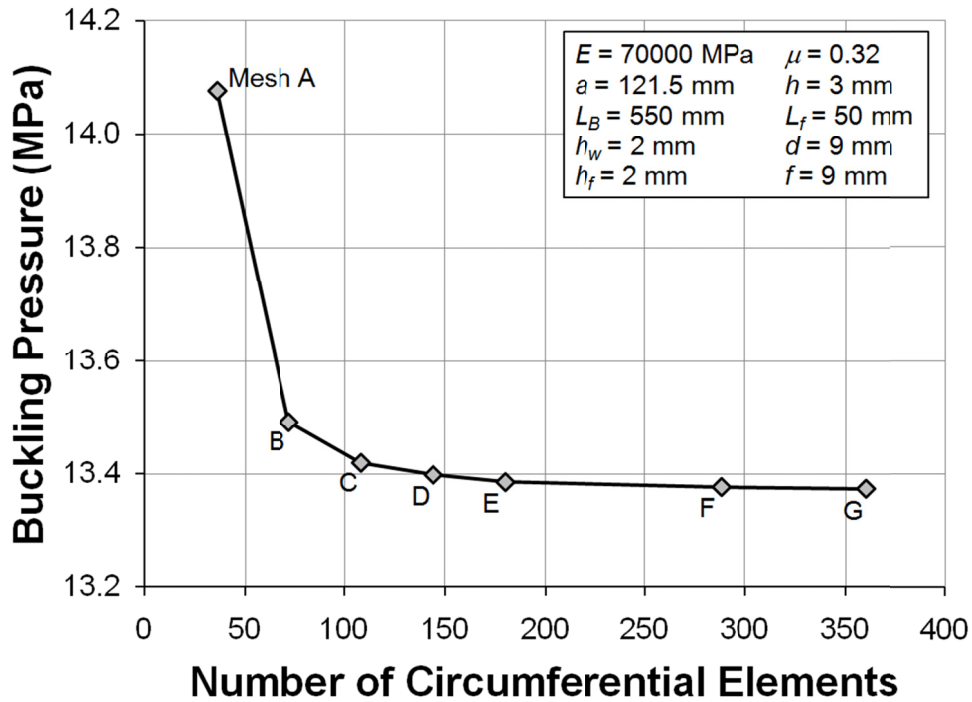


Figure 6: Results of a mesh convergence study for the elastic buckling of a simply-supported ring-stiffened cylinder under external pressure.

A mesh convergence study was performed for the FE model of the cylinder with $L_B L_f^{-1}=11$ and $d=f=9$ mm. The final FE mesh and predicted buckling mode for that configuration are shown in Figure 5. The results of the complete mesh convergence study are presented in Figure 6. Mesh F was chosen for final analysis of all the FE models, since it gave a buckling pressure within 0.2% of a model with half the mesh density (Mesh D).

The results of the verification study are shown in Figure 4, where the predicted buckling pressures are plotted against the ratio of cylinder length to stiffener spacing. The five sets of curves represent the five differently proportioned ring-stiffeners. The results for Kendrick's energy solution represent the minimum or critical buckling pressures, which were determined by iterating over a range of values for m and n .

As expected, the buckling pressure associated with a given ring-stiffener geometry decreases with cylinder length. Furthermore, each curve in Figure 4 can be seen to have an upper and lower bound with respect to buckling pressure. The lower bound on the right-hand side of each curve is approached as the cylinder length is increased, and is associated with the buckling strength of an infinitely long cylinder. The upper bound at the left of each curve is associated with the interframe buckling strength, which is the same for all of the cylinders since the shell thickness, stiffener spacing and cylinder radius are held constant for all models. Cylinders falling on the upper bound failed by interframe buckling with eight complete circumferential waves ($n=8$) and one half-wave between each stiffener ($m=N_f+1$, where N_f is the number of stiffeners). All other cylinders failed by overall buckling with one half-wave over the entire cylinder length ($m=1$). The discontinuities or kinks in the curves represent transitions in the circumferential wave number. The longer cylinders on the right side of the figure failed in an $n=2$ circumferential mode, while the other overall-critical cylinders failed in the $n=3$ or $n=4$ mode.

The FE results show close agreement with Kendrick's energy solution for cases of overall buckling. The FE-predicted upper bound associated with interframe buckling is approximately 15% greater than for the energy method results. That is likely related to Kendrick's assumptions that were discussed at the start of this section, especially his neglect of the support provided by the ring-stiffeners against interframe bending of the shell. Not surprisingly, the RMS error for this set of sixty analytical-numerical comparisons, at 7.8%, is much greater than for the first verification study. The RMS error is somewhat smaller, at 4.2%, when only the models failing by overall buckling are considered, likely because the torsional stiffness of the ring-stiffeners play a smaller role in overall buckling. The agreement was considered sufficient to verify the numerical implementation of the linear-elastic shell theory in the FE software, especially considering the close agreement found between FE and analytical models with nearly identical loading and geometry in the previous section. No attempts were made to more closely align the current FE models with Kendrick's assumptions.

2.3 Elasto-Plastic Collapse of a Ring-Frame

The final verification study was performed using Kendrick's nonlinear finite difference (FD) method for predicting the overall collapse pressure of a ring-stiffened cylinder [20]. With that method, a beam representing a single ring-stiffener and bay of plating is discretized in the circumferential direction, allowing OOC to be modeled. The beam cross-section is divided into a series of strips. In that way, residual stresses due to cold rolling can be applied as through-section

initial stresses, and furthermore, the incremental progression of yielding can be modeled. The current verification study did not consider residual stresses, since the validation test specimens in [15]-[17] were not cold rolled or welded.

Infinitely long cylinders were considered for this verification study in order to avoid the use of the associated correction factor in the FD model. Furthermore, the cylinder geometry was proportioned so that the ring-stiffeners were weak compared to the shell plating, which allowed “effective width” corrections for the shell plating to be turned off in the FD solution. The small ring-stiffeners also ensured an overall collapse, so that the interframe interaction correction that is sometimes applied to the FD model was not used. By negating the necessity of those correction factors, unnecessary discrepancies between the FE and FD models were eliminated.

The cylinder geometry and material properties are described in Figure 7. The axisymmetric geometry was the same for all models, while the yield stress, σ_y , and out-of-circularity magnitude were varied in order to generate a set of 30 unique cylinders. The OOC of all models was in the critical $n=2$ mode, and its magnitude is defined by the maximum radial eccentricity, e_{ps} , divided by the mid-plane shell radius, a . The material behaviour was assumed to be elastic-perfectly-plastic, with no strain hardening. The material law was straightforward for the FD beam model, since the stresses were one-dimensional. The FE model incorporated an isotropic von Mises yield surface for the two-dimensional stress field. Both types of numerical model incorporated isotropic hardening, thereby neglecting the Bauschinger effect.

Both the FD and FE models took advantage of symmetry, so that only one-quarter of the ring was modeled, with symmetry boundary conditions at the circumferential extents of the models. In the FE model, symmetry boundary conditions were also applied at the axial extents of the shell to simulate the infinite cylinder length. That was unnecessary for the FD beam model. 500 finite difference steps were used over the 90 degrees of circumference that was modeled. The plate thickness, web depth and flange thickness were each divided into 15 strips for stress calculations with the FD method.

All-shell FE models were used, even though the FD solution is based on beam theory, because, as mentioned above, the goal of the study is to verify shell models that will be used in the analysis of real structures. A mesh convergence study for the FE model led to the use of a mesh defined by 72 approximately square elements about the 90 degree arc, as shown in Figure 8 for a ring-frame with $\sigma_y=150$ MPa and $e_{ps}a^{-1}=0.1\%$. That mesh gave a collapse pressure within 0.2% of a mesh with half the density.

Only pressure loads on the shell plating were considered, since the FD beam model cannot account for axial loading. The axial loads that are normally applied to a shell FE model to account for forces transferred from end-caps or dome bulkheads were neglected. FD collapse pressures were arrived at by incrementally increasing the load until a converged solution could not be found. FE collapse pressures were calculated in a similar manner, using the modified Newton-Raphson method in a load control scheme. The minimum load increment was set at 0.0001 MPa for both the FD and FE analyses.

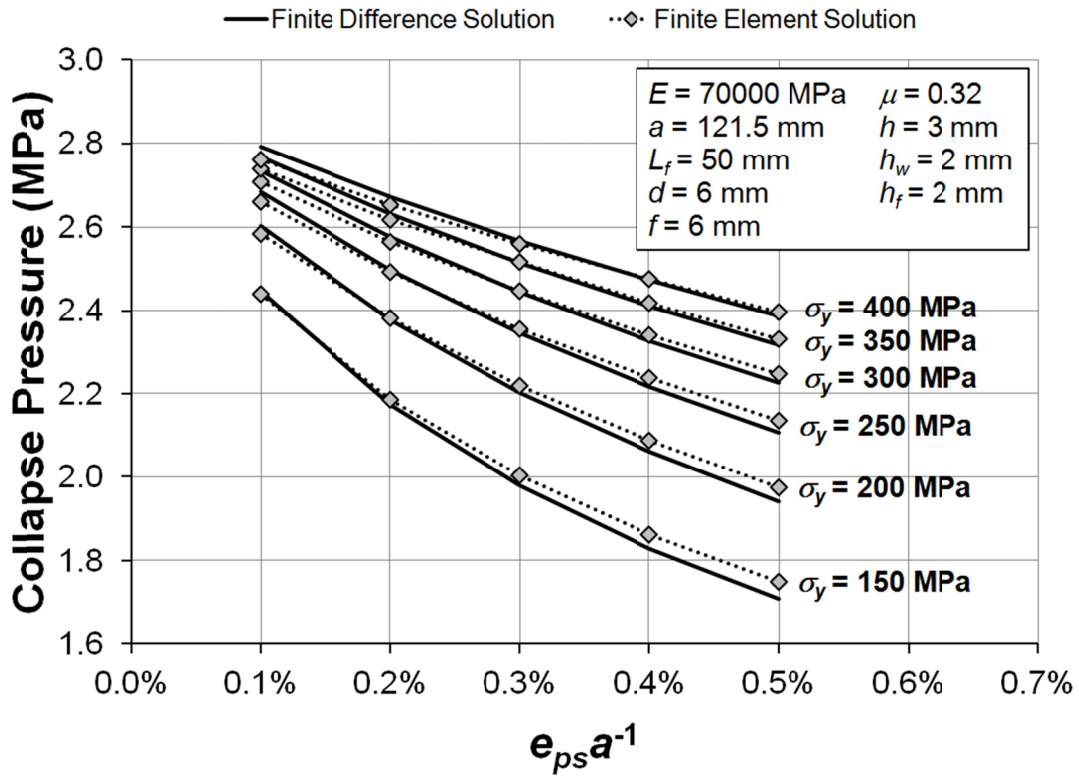


Figure 7: Results of a verification study based on the elasto-plastic overall collapse of an infinitely long ring-stiffened cylinder under external pressure.

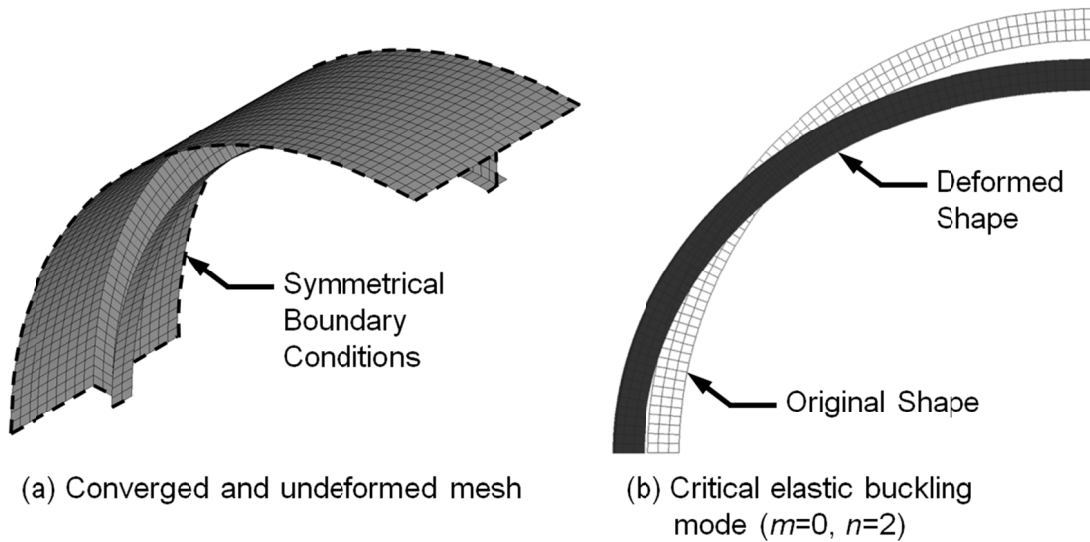


Figure 8: FE mesh (a) and predicted buckling mode (b) for a ring-frame with $\sigma_y=150 \text{ MPa}$ and $e_{ps}a^{-1}=0.1\%$.

The results of the verification study are presented in Figure 7, whereby the predicted elasto-plastic collapse pressures are plotted against the OOC magnitude. The FD solutions were generated using a DRDC in-house program called K79 [21]. The six sets of curves are associated with the six yield stresses that were studied. As expected, collapse pressures decreased as the yield stress was reduced and as the OOC magnitude was increased. The FD and FE solutions followed the same trends, with the greatest difference between the two sets of models being the rate of decline in the collapse pressure with OOC. That may be attributed to the two-dimensional stress field in the FE models, which delayed the onset of yielding compared to the one-dimensional stresses in the FD model. Nonetheless, the RMS error for the FE models, using the FD models as a benchmark, was less than 1%, a small value considering that the models were based on different structural theories.

3 Calculation Verification

Calculation verification was carried out in order to ensure that the following three aspects of the FE modeling were sufficiently refined: mesh density, load increment size, and the tolerances used to define convergence of the iterative solution at each load increment. Calculation verification is problem-specific; that is, the effects of the element mesh density and load increment size depend on the structural configuration and failure mode being studied. Because of that, calculation verification is performed on the numerical models that will be used for validation. By way of example, the following sections describe calculation verification that was performed for a specimen called L510-No18, which is briefly described below. A detailed description of that specimen is given in the experimental report in [16].

3.1 Example Test Specimen

The nominal axisymmetric geometry of specimen L510-No18 is shown in Figure 9. The ring-stiffened cylinder was fabricated by machining a tube of 6082-T6 aluminium on a CNC lathe. The shell and stiffeners were proportioned to induce failure by overall collapse. That failure mechanism was further encouraged by mechanically deforming the cylinder before testing in order to introduce out-of-circularity in the critical $m=1, n=3$ mode at an amplitude of approximately 0.4%. The specimen shape and shell thickness were measured before testing using a coordinate measuring machine. A graphical representation of the as-measured specimen OOC is shown in Figure 10. The yield strength of the aluminium, in the circumferential direction of the cylinder, was measured to be 305 MPa.

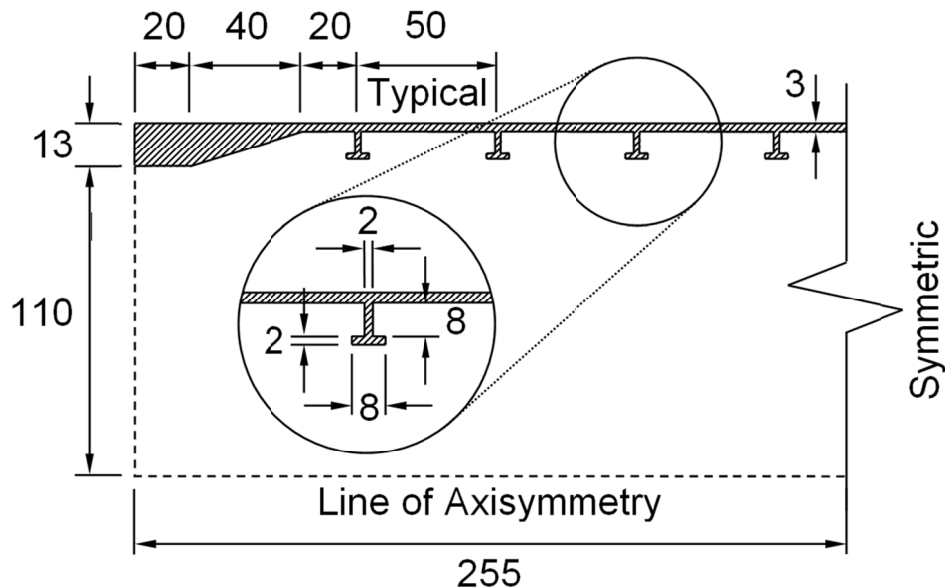


Figure 9: Nominal axisymmetric geometry of specimen L510-No18 [16]. All dimensions are in millimetres.

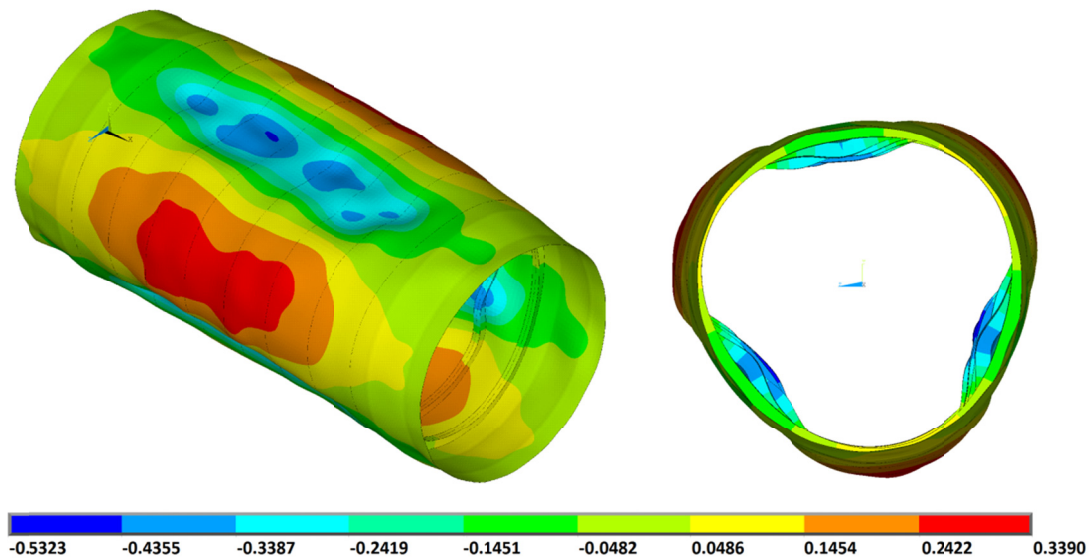


Figure 10: Graphical representation of out-of-circularity of specimen L510-No18. The colour contour maps describe the radial eccentricity (mm) based on a double Fourier analysis of the measurements of the outer shell taken by the CMM. The out-of-circularity is also indicated by the deformed shape of the model, whereby the imperfections are magnified by a factor of 50.



Figure 11: A photograph of specimen L510-No18 after collapse testing (left), and the collapse shape predicted using the standard FE methodology in Annex A.

End-caps were fixed to the cylinder ends with bolts, after which the specimen was loaded to collapse under external hydrostatic pressure in a pressure chamber. A series of strain gauges were used to estimate specimen deformations and stresses during testing, and the applied pressure was measured using pressure transducers. The collapse pressure was found to be 7.71 MPa, with the cylinder failing by overall elasto-plastic collapse in the expected $m=1, n=3$ mode. A photograph of the cylinder after testing is shown in Figure 11. The post-collapse deformations were concentrated at one of the $n=3$ collapse lobes.

The FE procedures for modeling the as-measured OOC and material properties, as well as generating the collapse prediction, are summarized in Annex A. Unless otherwise noted, all calculation verification analyses followed those FE modeling rules. The standard FE methodology gave a predicted collapse pressure of 8.08 MPa, over-predicting the experimental value by 4.7%. The FE-predicted collapse shape is shown in Figure 11.

3.2 Mesh Density

The mesh convergence study for L510-No18 covered three orders of magnitude with respect to the total number of nodes and elements in the mesh, as shown in Figure 12. A nonlinear analysis was performed for each mesh, with an initial load increment of 0.25 MPa (see Section 3.3) and a convergence tolerance set to 0.005 (see Section 3.4).

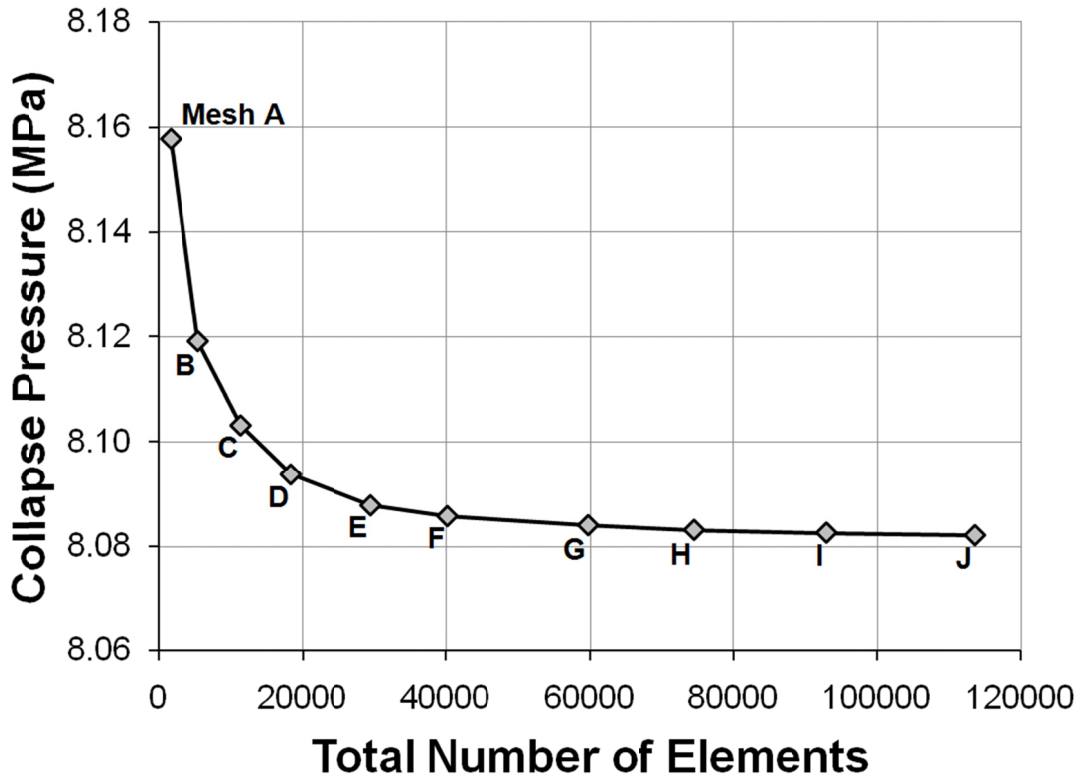


Figure 12: Results of a mesh convergence study for L510-No18, showing the predicted collapse pressure versus the total number of elements in the FE model.

In Figure 12, the predicted collapse pressure is plotted against the mesh density, as characterized by the total number of elements in the mesh. Each mesh was composed of a regular grid of approximately square shell elements. Mesh H was chosen for final analysis of L510-No18 and similar specimens in [15]-[17]. The predicted collapse pressure associated with that mesh was within 0.13% of the predicted strength for Mesh D, which had half the mesh density. Furthermore, the collapse pressure for Mesh H was only 0.001 MPa greater than the two densest meshes studied. Mesh H is characterized by 288 elements about the circumference of the cylinder, 19 elements between frames, and 4 elements on both the stiffener web and flange. The FE model shown in Figure 11 used Mesh H.

3.3 Load Increment Size

The current verification study looked at the sensitivity of the predicted collapse pressure to the size of the first load increment, which was varied between 0.0625 and 2 MPa. L510-No18 was used for the case study, with the converged Mesh H and a solution convergence tolerance of 0.005 (see Section 3.4).

The six cases of load increment size are summarized in Table 1, along with the associated collapse pressures predicted by the FE models. With each analysis, the initial load increment size was specified, after which the arc length method and automatic time-stepping routine in ANSYS controlled the load application. Those algorithms forced the nonlinear solution increments to become smaller and smaller as the analysis progressed, so that the final load increment at the collapse pressure was only a fraction of the initial value. Table 1 also lists the size of the last load increment before collapse. It can be seen that, in general, the size of the last load increment decreases as the initial load increment is reduced. That is largely due to the use of the arc length method, which enforces a constant length in load-displacement space. That effect can be seen in Figure 13, which shows the predicted pressure-displacement curve associated with an initial load increment of 1.0 MPa. Table 1 also lists the total number of load increments required to reach the collapse pressure for each case.

Table 1: Summary of a load increment study for L510-No18.

Model	Load Increment Size (MPa)		Load Increments to Collapse	Collapse Pressure (MPa)
	Initial	Last Increment before Collapse		
L1	2.0000	0.0165	6	8.0772
L2	1.0000	0.0128	11	8.0755
L3	0.5000	0.0204	21	8.0825
L4	0.2500	0.0067	42	8.0831
L5	0.1250	0.0006	85	8.0841
L6	0.0625	0.0001	170	8.0844

The load increment study is summarized graphically in Figure 14, where the predicted collapse pressure is plotted as a function of the total number of increments to collapse. The load increment size associated with a given number of increments to collapse is plotted on the secondary axis. It was found that the load increment size affects the collapse pressure prediction primarily through its relationship with the total number of load increments to collapse. Larger load increment sizes result in a smaller number of load increments in total. That may affect the nonlinear solution by increasing the incremental plastic strain, but more importantly, large load increments lead to large load-displacement arcs, whereby the peak load can be “stepped over” when using the arc length method. That error is reduced with the size of the load-displacement increments.

Despite the apparent trends described above, the nonlinear collapse prediction was not found to be very sensitive to load increment size. The variation in predicted collapse pressures over the three orders of magnitude of load increment size studied here was within 0.1% for all cases. That insensitivity is likely due to the automatic time-stepping routine, which reduces the load increment size when the solution becomes highly nonlinear at the onset of yielding and collapse. Nonetheless, the collapse prediction could be more sensitive to load increment size in cases where the peak in the pressure-displacement curve is sharper, because the arc-length method may be more likely to step over the maximum pressure.

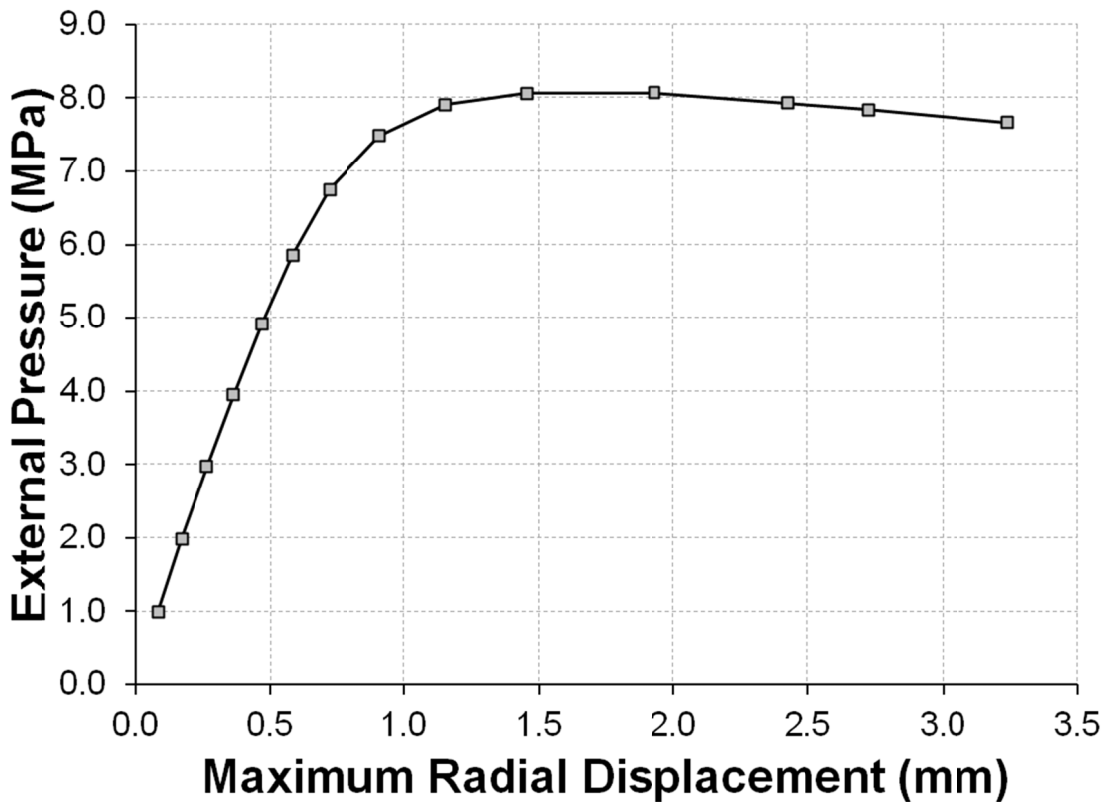


Figure 13: Pressure-displacement curve predicted by nonlinear FE analysis for L510-No18. The FE model is based on Mesh H, with an initial load increment of 1.0 MPa. The plotted displacement corresponds with the maximum deformation for the predicted collapse shape.

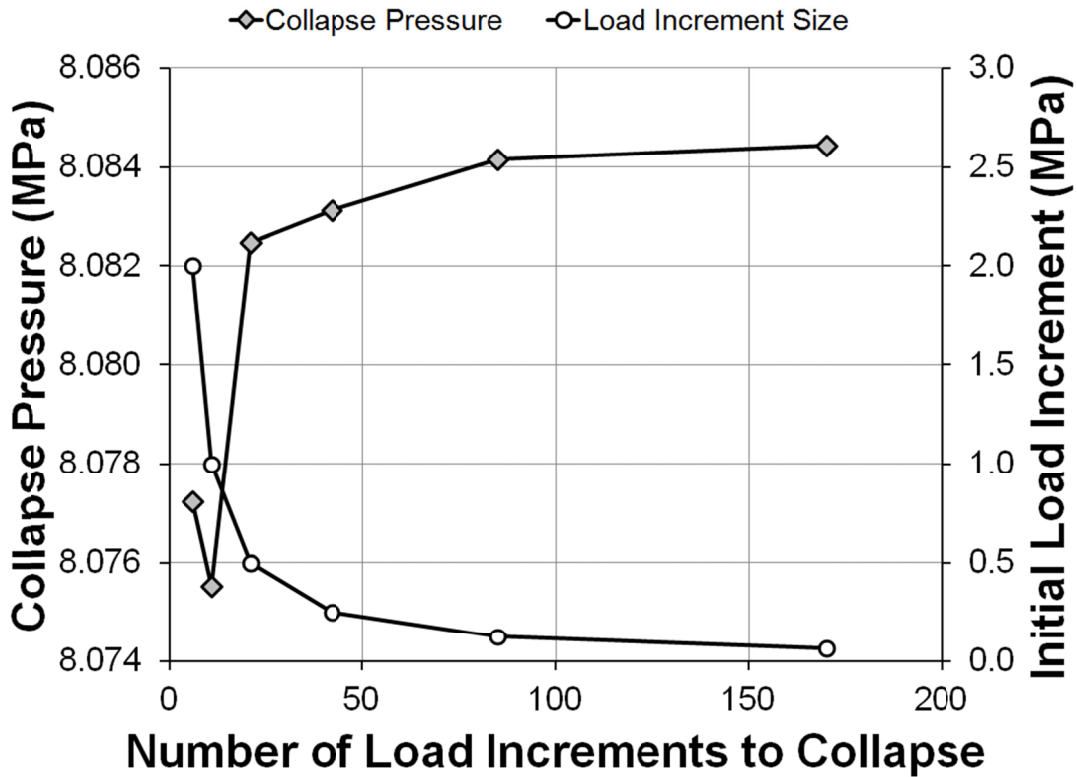


Figure 14: Results of a load increment size study for L510-No18, showing the predicted FE collapse pressure versus the total number of load increments up to the collapse pressure. The initial load increment size corresponding with each analysis is shown on the secondary axis.

The load increment size of 0.25 MPa, corresponding with 42 load increments to collapse, was considered to be converged, since its collapse prediction was within 0.1% of the value for an analysis with twice the increment size. That case will be used in all further analyses in the validation study. From a more general perspective, this verification study suggests that the initial load increment should be approximately 3% of the collapse pressure of the hull structure being analyzed. That recommendation is valid as long as an arc length method is used, and the arc length value is not allowed to exceed the initial value. The analyst may use the FD method discussed in Section 2.3, or the empirical design curve from [1], to estimate the collapse pressure of a particular hull before the FE prediction is made. In that way a sufficiently small load increment can be determined beforehand, without resorting to a complete verification study.

3.4 Solution Convergence Tolerances

With the ANSYS analyses described herein, the solution at each load increment was considered to be converged if the L2 norm of the residual force vector was less than the norm of the applied force vector times a convergence tolerance. The L2, or Euclidean, norm is taken as the square root of the sum of the squares of each vector value [4]. As mentioned above, the typical value for the convergence tolerance was 0.005. In the current verification study, the collapse pressure for

L510-No18 was predicted using convergence tolerances varying over three orders of magnitude, from 0.0005 to 0.02. Each analysis used Mesh H, as described in Section 3.2, and an initial load increment of 0.25 MPa, based on the analyses described in Section 3.3.

It was found that the convergence tolerance, within the range studied here, did not affect the predicted collapse pressure at all; that is, all analyses yielded the same collapse pressure. That insensitivity was due to the use of a converged mesh and, especially, load increment size. With small load increments, the overall response, which is significantly nonlinear (see Figure 13), was broken down into small load-displacement increments that were nearly linear. That allowed the Newton-Raphson iteration scheme to achieve good convergence after only the minimum two iterations that are required by the algorithm. The convergence tolerance was never exceeded in the pre-collapse predictions for any of the cases studied, and did not therefore play a role in the results. When the study was repeated using a larger load increment size of 2.0 MPa, the convergence tolerance was exceeded in some of the analyses, but the resulting collapse pressures were nearly identical, within 0.2% of each other. The default tolerance of 0.005 was found to be more than sufficient for further V&V analyses.

4 Conclusions

Code verification showed that the benchmark and FE solutions are in excellent agreement when they are based on the same theory and assumptions. The discrepancy between the benchmark and numerical solutions increased with the complexity of the test problems. That “error” does not imply that the numerical models have been incorrectly implemented, because the reliability of the benchmark solutions themselves decreases with the problem complexity. With the most realistic models involving elasto-plastic collapse and out-of-circularity imperfections, the underlying structural theory was not even the same for the benchmark and numerical models. Good agreement between those models was found nonetheless. The various discrepancies between the benchmark and numerical models have been attributed to short-comings of the former solutions, or to unavoidable differences in the underlying theory of the two sets of models. Despite those differences, the numerical models showed good agreement with the benchmarks over a range of structural configurations and failure modes. It is concluded that the results presented herein verify that the numerical algorithms have been correctly implemented in the CylMesh and ANSYS programs.

The calculation verification studies presented here are meant to demonstrate that the validation numerical models are sufficiently refined, in all respects, to yield the “exact” solution to the underlying equations (but not necessarily the correct solution of the problem being studied) with sufficient precision. The collapse prediction was shown to be more sensitive to the mesh density than to either the load increment size or the convergence tolerance. When a converged mesh and load increment were used, the solution was completely insensitive to the convergence tolerance. That is due to the highly linearized incremental response associated with dense meshes and small load increments. Because calculation verification investigations are somewhat tedious and time-consuming, they are often overlooked by the analyst. That neglect can lead to unnecessary errors in the numerical prediction. The current work has generated generally applicable values for load increment size (3% of the collapse pressure) and convergence tolerance (0.5%), which may be used for future FE collapse predictions; however, a mesh convergence study must be performed each time a new structural and loading configuration is considered.

The verification studies described herein provide assurance that the Cylmesh and ANSYS software, which are frequently used by DRDC to assess the pressure hulls, have correctly implemented the underlying mathematical and physical models required to predict hull collapse. However, verification of numerical models is only the first step in a V&V procedure. DRDC has also completed the more resource intense validation work, including the experiments in [12]-[17], and the numerical simulations of those test specimens using CylMesh/ANSYS in [10], [16] and [17]. What remains to be done is to derive a PSF for FE analysis of pressure hulls using a statistical analysis of the experimental-numerical comparisons, as suggested in [2].

References

- [1] DPA (2001). SSP74 Design of Submarine Structures. United Kingdom: Defence Procurement Agency, Sea Technology Group.
- [2] MacKay, J.R., van Keulen, F., and Smith, M.J. (2011). Quantifying the accuracy of numerical collapse predictions for the design of submarine pressure hulls. *Thin-Walled Structures*, 49, 145-156.
- [3] ASME (2006). ASME V&V 10-2006: Guide for Verification and Validation in Computational Solid Mechanics. American Society of Mechanical Engineers (ASME), New York.
- [4] SAS IP Inc. (2007). ANSYS release 11.0 documentation. SAS IP Inc., Canonsburg.
- [5] Martec Limited (2004). SubSAS: An Integrated Suite of Submarine Structural Analysis Codes User's Manual. (Martec SM-04-14). Martec Limited, Halifax.
- [10] Martec Limited. (2008). VAST User's Manual, Version 8.8. Martec Limited, Halifax.
- [11] MacKay, J.R., Jiang, L., and Glas, A.H. (2011). Accuracy of nonlinear finite element collapse predictions for submarine pressure hulls with and without artificial corrosion damage. DRDC Atlantic SL 2010-314. *Marine Structures*, 24, 292-317.
- [12] MacKay, J.R. (2007). Experimental investigation of the strength of damaged pressure hulls – Phase 1. (DRDC Atlantic TM 2006-304). Defence Research and Development Canada – Atlantic.
- [13] MacKay, J.R. (2007). Experimental investigation of the strength of damaged pressure hulls – Phase 2, Summary of experimental results. (DRDC Atlantic TM 2007-013). Defence Research and Development Canada – Atlantic.
- [14] MacKay, J.R. (2008). Experimental investigation of the strength of damaged pressure hulls – Phase 3. (DRDC Atlantic TM 2008-093). Defence Research and Development Canada – Atlantic.
- [15] MacKay, J.R. (2010). Experimental investigation of the strength of damaged pressure hulls – Phase 4: The influence of material properties on pressure hull collapse. (DRDC Atlantic TM 2009-299). Defence Research and Development Canada – Atlantic.
- [16] MacKay, J.R. (2011). Experimental investigation of the strength of damaged pressure hulls – Phases 5 & 6: The influence of out-of-circularity on collapse. (DRDC Atlantic TM 2010-239). Defence Research and Development Canada – Atlantic.
- [17] MacKay, J.R. (2011). Experimental investigation of the strength of damaged pressure hulls – Phase 7: The interaction of multiple corrosion damage cases. (DRDC Atlantic TM 2011-034). Defence Research and Development Canada – Atlantic.

- [18] von Mises, R. (1929). The critical external pressure of cylindrical tubes under uniform radial and axial load. *Stodola's Festschrift*, 418-430.
- [19] Kendrick, S. (1953). The buckling under external pressure of circular cylindrical shells with evenly spaced equal strength circular ring frames – Part I. (NCRE Report No. R.211). Naval Construction Research Establishment.
- [20] Kendrick, S. (1979). The Influence of Shape Imperfections and Residual Stress on the Collapse of Stiffened Cylinders. In *Proceedings of the Conference on Significance of Deviations from Design Shape*, 25-35. I. Mech. E.
- [21] Smith, M.J. and MacKay, J.R. (2004). Overall Elasto-Plastic Collapse of Submarine Pressure Hull Compartments. (DRDC Atlantic TM 2004-243). Defence Research and Development Canada – Atlantic.

Annex A Standard Numerical Methodology

Finite element models were generated using CylMesh and analyzed using ANSYS 11.0 [4]. The FE meshes modeled the full extent of each cylinder and consisted of 4-node finite strain shell elements (ANSYS element “SHELL181”) with four in-plane (full integration) and five through-thickness integration points. Each FE model was composed of approximately square shell elements in a regular grid, so that the mesh density was uniform over the entire cylinder. A uniform external pressure load was applied to the shell of each model, with equivalent edge pressures at the cylinder ends to represent the axial load transferred from, for example, specimen end caps.

Elasto-plastic collapse pressures were predicted with ANSYS using nonlinear quasi-static analysis, including large displacements and material plasticity. Geometric nonlinearities were captured with an updated Lagrangian formulation in combination with a co-rotational system. Loads were applied incrementally, and the follower-force effect, which arises from the changing direction of pressure loads with displacements, was accounted for. The solution at each load increment was arrived at through a modified Newton-Raphson approach to iteratively balancing the internal and external forces.

The arc length method was used in order to allow the validation analyses to be carried past limit points and into the post-collapse regions. Load application was controlled by specifying the initial load increment size for the arc length method. After that, the arc length method and an automatic time-stepping algorithm in ANSYS were used to control the load application. The arc length was not permitted to increase beyond the initial value, which resulted in smaller and smaller load increments as the nonlinear analyses progressed. Furthermore, the automatic time-stepping algorithm automatically reduced the arc length if a converged solution could not be found at a given load increment. The predicted collapse pressure was taken as the maximum limit point in the numerical load-displacement curve.

The following aspects of the FE modeling apply only to simulations of test specimens. Nonlinear maps of out-of-circularity imperfections and shell thicknesses were derived through double Fourier series decompositions of the shape measurement data. Those maps were applied to the nodal positions and shell elements of the initially shape-perfect FE models. Stress-strain curves for FE analysis were generated by averaging the measured engineering curves for coupons taken from the circumferential direction of each test specimen. The resulting engineering curves were used to generate true stress-strain curves, which were implemented via multi-linear material models with isotropic von Mises yield surfaces and kinematic hardening. The end-caps used in the experiments were not explicitly modeled. Instead, the support provided to the cylinders by the end-caps was implicitly modeled by simply supporting the FE models at the cylinder ends and at the intersection of the thick end rings with the tapered shell section. Those boundary conditions resulted in a “quasi-clamped” constraint whereby out-of-plane bending was prevented at the cylinder ends, while end-warping was allowed.

This page intentionally left blank.

List of symbols/abbreviations/acronyms/initialisms

a	mid-plane radius of cylindrical shell
ASME	American Society of Mechanical Engineers
CNC	computer numerical controlled
d	depth of ring-stiffener web
DND	Department of National Defence
DRDC	Defence Research & Development Canada
DRDKIM	Director Research and Development Knowledge and Information Management
e	relative error
e_{ps}	maximum radial eccentricity
E	Young's modulus
f	breadth of ring-stiffener flange
FD	finite difference
FE	finite element
h	thickness of a cylindrical shell
h_f	thickness of ring-stiffener flange
h_w	thickness of ring-stiffener web
L	length of a cylindrical shell
L_B	length of a ring-stiffened cylinder
L_f	stiffener spacing
m	number of half-waves over the length of a cylinder
mm	millimetre
MPa	megaPascal
n	number of complete waves around the circumference of a cylinder
N	number of analytical-numerical comparisons
N_f	number of ring-stiffeners
OOC	out-of-circularity
P_{cl}	classical analytical buckling pressure
P_{FE}	finite element buckling pressure
P_{m1}	von Mises pressure

PSF	partial safety factor
R&D	Research & Development
RMS	root mean square
StDev	standard deviation
V&V	verification and validation
μ	Poisson's ratio
σ_y	yield stress

Distribution list

Document No.: DRDC Atlantic TM 2011-281

LIST PART 1: Internal Distribution by Centre

- 4 Author (2 paper copies, 2 CDs)
- 3 DRDC Atlantic Library (1 paper copy, 2 CDs)

- 7 TOTAL LIST PART 1

LIST PART 2: External Distribution by DRDKIM

- 1 Library and Archives Canada, Attn: Military Archivist, Government Records Branch
- 1 NDHQ/DMEPM(SM) 4-2
- 1 Prof. Fred van Keulen
Department of Precision and Microsystems Engineering
Faculty 3mE
Delft University of Technology
Office 4B-1-32
Mekelweg 2
2628 CD Delft
THE NETHERLANDS
- 1 NDHQ/DRDKIM 3 (1 CD)

- 4 TOTAL LIST PART 2

11 TOTAL COPIES REQUIRED

This page intentionally left blank.

DOCUMENT CONTROL DATA

(Security classification of title, body of abstract and indexing annotation must be entered when the overall document is classified)

1. ORIGINATOR (The name and address of the organization preparing the document. Organizations for whom the document was prepared, e.g. Centre sponsoring a contractor's report, or tasking agency, are entered in section 8.) Defence R&D Canada – Atlantic 9 Grove Street P.O. Box 1012 Dartmouth, Nova Scotia B2Y 3Z7		2. SECURITY CLASSIFICATION (Overall security classification of the document including special warning terms if applicable.) UNCLASSIFIED (NON-CONTROLLED GOODS) DMC A REVIEW: GCEC JUNE 2010	
3. TITLE (The complete document title as indicated on the title page. Its classification should be indicated by the appropriate abbreviation (S, C or U) in parentheses after the title.) Verification of Numerical Models for Pressure Hull Collapse Predictions			
4. AUTHORS (last name, followed by initials – ranks, titles, etc. not to be used) MacKay, J.R.			
5. DATE OF PUBLICATION (Month and year of publication of document.) November 2011		6a. NO. OF PAGES (Total containing information, including Annexes, Appendices, etc.) 40	6b. NO. OF REFS (Total cited in document.) 21
7. DESCRIPTIVE NOTES (The category of the document, e.g. technical report, technical note or memorandum. If appropriate, enter the type of report, e.g. interim, progress, summary, annual or final. Give the inclusive dates when a specific reporting period is covered.) Technical Memorandum			
8. SPONSORING ACTIVITY (The name of the department project office or laboratory sponsoring the research and development – include address.) Defence R&D Canada – Atlantic 9 Grove Street P.O. Box 1012 Dartmouth, Nova Scotia B2Y 3Z7			
9a. PROJECT OR GRANT NO. (If appropriate, the applicable research and development project or grant number under which the document was written. Please specify whether project or grant.) 11gh04		9b. CONTRACT NO. (If appropriate, the applicable number under which the document was written.)	
10a. ORIGINATOR'S DOCUMENT NUMBER (The official document number by which the document is identified by the originating activity. This number must be unique to this document.) DRDC Atlantic TM 2011-281		10b. OTHER DOCUMENT NO(s). (Any other numbers which may be assigned this document either by the originator or by the sponsor.)	
11. DOCUMENT AVAILABILITY (Any limitations on further dissemination of the document, other than those imposed by security classification.) Unlimited			
12. DOCUMENT ANNOUNCEMENT (Any limitation to the bibliographic announcement of this document. This will normally correspond to the Document Availability (11). However, where further distribution (beyond the audience specified in (11) is possible, a wider announcement audience may be selected.) Unlimited			

13. **ABSTRACT** (A brief and factual summary of the document. It may also appear elsewhere in the body of the document itself. It is highly desirable that the abstract of classified documents be unclassified. Each paragraph of the abstract shall begin with an indication of the security classification of the information in the paragraph (unless the document itself is unclassified) represented as (S), (C), (R), or (U). It is not necessary to include here abstracts in both official languages unless the text is bilingual.)

The verification aspects of a verification and validation (V&V) study for the numerical modeling of the collapse of pressure hulls are described. A series of finite element (FE) analyses were performed using ANSYS in order to verify that the numerical methodology was correctly implemented in the software (code verification) and that spatial and temporal refinement of validation FE models of test specimens were adequate (calculation verification). FE predictions of elastic and inelastic buckling pressures for 140 cylinders and ring-frames under external pressure were found to be within 8%, on average, of the benchmark analytical or numerical solutions. The FE error was attributed to unavoidable differences between the numerical and benchmark models, rather than problems with the FE software, so that code verification was considered to have been achieved. With calculation verification, the nonlinear FE solution was found to be most sensitive to the spatial refinement associated with the mesh density. Load increment size was found to affect the collapse prediction to a lesser extent, and the tolerance used to define convergence of the incremental solution did not affect the collapse prediction at all when a refined mesh and load increment were used. The outcomes of the calculation verification study were a standard mesh density, load increment size and convergence tolerance that can be used for further validation analyses of test specimens, and for future FE analyses of pressure hulls.

Les aspects de vérification d'une étude de vérification et de validation (V et V) pour la modélisation numérique de l'écrasement de coques épaisses sont décrits. Une série d'analyses par éléments finis ont été effectuées à l'aide du logiciel ANSYS dans le but de vérifier si la méthodologie numérique a bien été implantée dans le logiciel (vérification des codes) et si le raffinement spatial et le raffinement temporel des modèles de validation par éléments finis des spécimens d'essais étaient adéquats (vérification des calculs). Les prédictions par éléments finis des pressions de flambage élastique et inélastique pour 140 cylindres et cadres de fuselage sous pression externe sont d'environ 8 %, en moyenne, des solutions analytiques ou numériques de référence. L'erreur par éléments finis a été attribuée à des différences inévitables entre les modèles numériques et les modèles de référence, plutôt qu'à des problèmes avec le logiciel d'analyse par éléments finis, ce qui fait en sorte que la vérification des codes a été considérée comme effectuée. Avec la vérification des calculs, la solution d'éléments finis non linéaire a été jugée la plus sensible pour le raffinement spatial associé à la densité de mailles. Il a été déterminé que la variation de charge a une faible incidence sur la prédiction d'écrasement et que la tolérance utilisée pour définir la convergence de la solution de variation n'a aucune incidence sur la prédiction d'écrasement lorsqu'un maillage raffiné et une variation de charge sont utilisés. Les résultats de l'étude de vérification des calculs étaient une densité des mailles standard, une variation de la charge standard et une tolérance de convergence standard, qui peuvent être utilisées pour de futures analyses de validation des spécimens d'essais et pour de futures analyses par éléments finis de coques épaisses.

14. **KEYWORDS, DESCRIPTORS or IDENTIFIERS** (Technically meaningful terms or short phrases that characterize a document and could be helpful in cataloguing the document. They should be selected so that no security classification is required. Identifiers, such as equipment model designation, trade name, military project code name, geographic location may also be included. If possible keywords should be selected from a published thesaurus, e.g. Thesaurus of Engineering and Scientific Terms (TEST) and that thesaurus identified. If it is not possible to select indexing terms which are Unclassified, the classification of each should be indicated as with the title.)

pressure hull; finite element analysis; buckling; collapse; verification; validation; V&V

This page intentionally left blank.

Defence R&D Canada

Canada's leader in defence
and National Security
Science and Technology

R & D pour la défense Canada

Chef de file au Canada en matière
de science et de technologie pour
la défense et la sécurité nationale



www.drdc-rddc.gc.ca